"Complete" gravitational waveforms for black-hole binaries with non-precessing spins

P. Ajith,[1,2,3] M. Hannam,[4,5] S. Husa,[6] Y. Chen,[2] B. Brügmann,[7] N. Dorband,[8]
D. Müller,[7] F. Ohme,[8] D. Pollney,[8] C. Reisswig,[8] L. Santamaría,[8] and J. Seiler[8]

[1]*LIGO Laboratory, California Institute of Technology, Pasadena, CA 91125, USA*
[2]*Theoretical Astrophysics, California Institute of Technology, Pasadena, CA 91125, USA*
[3]*Max-Planck-Institut für Gravitationsphysik (Albert-Einstein-Institut), Callinstr. 38, 30167 Hannover, Germany*
[4]*Physics Department, University College Cork, Cork, Ireland*
[5]*Gravitational Physics, Faculty of Physics, University of Vienna, Boltzmanngasse 5, A-1090 Vienna, Austria*
[6]*Departament de Física, Universitat de les Illes Balears, Crta. Valldemossa km 7.5, E-07122 Palma, Spain*
[7]*Theoretisch-Physikalisches Institut, Friedrich Schiller Universität Jena, Max-Wien-Platz 1, 07743 Jena, Germany*
[8]*Max-Planck-Institut für Gravitationsphysik (Albert-Einstein-Institut), Am Mühlenberg 1, 14476 Golm, Germany*

(Dated: March 10, 2010)

We present the first analytical inspiral-merger-ringdown gravitational waveforms from black-hole (BH) binaries with non-precessing spins. By matching a post-Newtonian description of the inspiral to a set of numerical calculations performed in full general relativity, we obtain a waveform family with a conveniently small number of physical parameters. The physical content of these waveforms includes the "orbital hang-up" effect, when BHs are spinning rapidly along the direction of the orbital angular momentum. These waveforms will allow us to detect a larger parameter space of BH binary coalescence, to explore various scientific questions related to GW astronomy, and could dramatically improve the expected detection rates of GW detectors.

Introduction.— Coalescing black-hole (BH) binaries are among the most promising candidate sources for the first direct detection of gravitational waves (GWs). Such observations will lead to precision tests of the strong-field predictions of general relativity as well as provide a wealth of information relevant to fundamental physics, astrophysics, and cosmology [1]. Computation of the expected waveforms from such sources is a key goal in current gravitational research.

While the *inspiral* and *ring-down* stages of the BH coalescence are well-modeled by perturbative techniques, an accurate description of the *merger* requires numerical solutions of Einstein's equations. Although performing numerical simulations over the entire parameter space of BH coalescence is computationally prohibitive, waveform templates modeling all three stages of BH coalescence can now be constructed by combining analytical- and numerical-relativity results, dramatically improving the sensitivity of searches for GWs from BH binaries, and the accuracy of estimating the source parameters [2, 3, 4, 5]. To date, "complete" inspiral-merger-ringdown (IMR) templates have been computed only for nonspinning BH binaries [2, 4, 5, 6, 7], which are effectively employed in GW searches, and in a number of astrophysical studies (see, e.g., [8, 9, 10]). However, nonspinning BHs are expected to be astrophysically rare, and most BHs in nature may be highly spinning [11, 12, 13]. This necessitates the inclusion of spinning-binary waveforms in detector searches. But, spin adds six parameters to the parameter space (three for the spin vector of each BH), and each additional parameter in a search template bank leads to a higher signal-to-noise-ratio (SNR) threshold for a confident detection [14]. Most importantly, this requires sufficiently accurate numerical simulations across this large parameter space, which are not yet available.

In this letter, we present an IMR waveform family modeling the dominant harmonic of binaries with non-precessing spins (i.e., spins parallel/anti-parallel to the orbital angular momentum). Our waveforms will significantly improve the "distance reach" of present and future GW detectors and will facilitate various astrophysical studies. Aligned-spin binaries are an astrophysically interesting population as such systems are expected from isolated binary evolution and in gas-rich galactic mergers [15, 16, 17]. Such systems also exhibit important strong-gravity effects like the "orbital hang-up". We make use of the degeneracies in the physical parameters to parametrize our waveform family by only the total mass $M \equiv m_1 + m_2$ of the binary, the symmetric mass ratio $\eta \equiv m_1 m_2/M^2$, and a *single* spin parameter $\chi \equiv (1+\delta)\,\chi_1/2 + (1-\delta)\,\chi_2/2$, where $\delta \equiv (m_1 - m_2)/M$ and $\chi_i \equiv S_i/m_i^2$, S_i being the spin angular momentum of the ith BH (compare also [18]). The last feature is motivated by the observation (see e.g., [19]) that the leading spin-orbit-coupling term in post-Newtonian waveforms is dominated by this parameter.

Numerical simulations.— the Binary BH (BBH) waveforms covering at least eight cycles before merger were produced by solving the full Einstein equations numerically, as written in the "moving-puncture" 3+1 formulation [20, 21]. The numerical solutions were calculated with the `BAM` [22, 23] and `CCATIE` [24] codes, starting with initial data that model BHs with conformally flat punctures [25, 26]. Initial momenta were chosen to give low-eccentricity inspiral, using either an extension of the method described in [27], or the quasicircular formula used in [28]. GWs were extracted at $R_{ex} = 90M$ with `BAM` and $R_{ex} = 160M$ with `CCATIE`, using the procedures discussed in [22, 24]. In all simulations the GW amplitude is accurate to within at least 10% and the phase accurate to within at least 1 radian over the duration of the simulation. Studies in the equal-mass nonspinning case suggest that these waveforms are within the accuracy requirements for both GW detection and source parameter estimation with the current detectors [29].

Five sets of simulations were used in this paper: (1) Equal-mass binaries with spins equal and parallel to the binary's orbital angular momentum, with $\chi_i = \pm\{0.25, 0.5, 0.75, 0.85\}$. The simulations with positive spins (the "orbital hang-up case") are described in detail in [30], and those with negative spins will be described further in [31]. (2) The same general non-precessing spin configuration, but using *unequal-mass* binaries with $q \equiv m_1/m_2 = \{2, 2.5, 3\}$ and $\chi_i = \{\pm 0.5, 0.75\}$. (3) Non-spinning binaries with $q = \{1, 1.5, 2, 2.5, 3, 3.5, 4\}$. (4) Unequal-

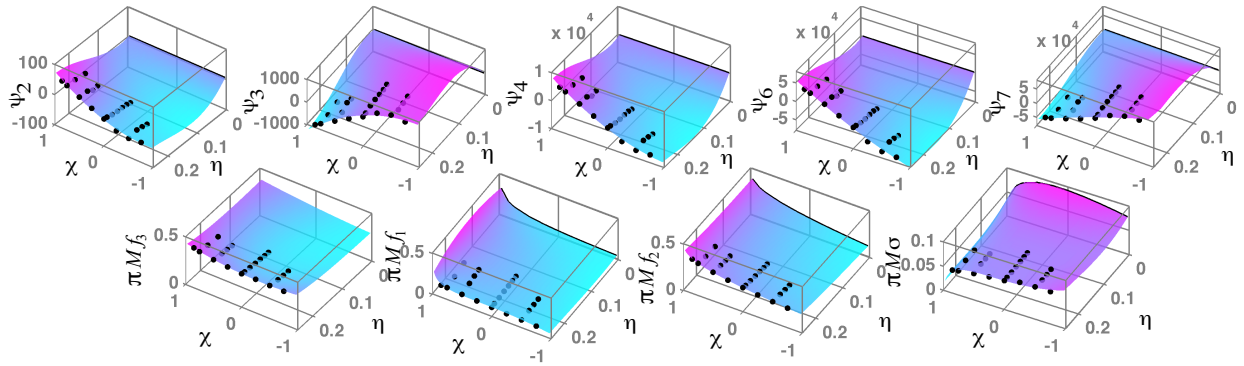

FIG. 1: Phenomenological parameters ψ_k, f_1, f_2, f_3 and σ computed from the *equal-spin* hybrid waveforms (dots), and the analytical fits given by Eq. (2) (surfaces). Test-mass limit is indicated by black traces. η is the symmetric mass ratio and χ is the spin parameter.

mass, unequal-spin binaries with $q = \{2,3\}$ and $(\chi_1,\chi_2) = (-0.75, 0.75)$. (5) Equal-mass, unequal-spin binaries with $\chi_i = \pm\{0.2, 0.3, 0.4, 0.6\}$. The simulation sets (1)–(4) were performed with the BAM code, while set (5) was performed with the CCATIE code. The analytical waveform family is constructed *only* employing the equal-spin simulation sets (1)–(3), while sets (4) and (5) were used to test the efficacy of the template family to model the expected signals from more general spin/mass configurations.

Constructing hybrid waveforms.— Following [2, 6], we produce a set of "hybrid waveforms" by matching post-Newtonian (PN) and numerical-relativity (NR) waveforms in an overlapping time interval $[t_1, t_2]$. These hybrids are assumed to be the target signals that we want to detect. For the PN inspiral waveforms we choose the "TaylorT1" approximant [32] waveforms at 3.5PN [33] phase accuracy. This is motivated by PN-NR comparisons of equal-mass spinning binaries, in which the accuracy of the TaylorT1 approximant was found to be the most robust [30, 31]. We include the 3PN amplitude corrections to the dominant quadrupole mode [34] and the 2.5PN spin-dependent corrections [19], which greatly improved the agreement between PN and NR waveforms.

If $\mathrm{h}(t) = h_+(t) - \mathrm{i}h_\times(t)$ denotes the time-domain waveform from a binary, we match the PN and NR waveforms by doing a least-square fit over time and phase shifts between the waveforms, and a scale factor a that reduces the PN-NR amplitude difference. The NR waveforms are combined with the "best-matched" PN waveforms in the following way: $\mathrm{h}^{\rm hyb}(t) \equiv a\tau(t)\,\mathrm{h}^{\rm NR}(t) + (1-\tau(t))\,\mathrm{h}^{\rm PN}(t)$, where τ ranges linearly from zero to one for $t \in [t_1, t_2]$.

Waveform templates for non-precessing binaries.— The analytical waveforms that we construct can be written in the Fourier domain as $h(f) \equiv A(f)\, e^{-\mathrm{i}\Psi(f)}$, where

$$A(f) \;\equiv\; C f_1^{-7/6} \begin{cases} f'^{-7/6}\,(1+\sum_{i=2}^{3}\alpha_i\, v^i) & \text{if } f < f_1 \\ w_m\, f'^{-2/3}\,(1+\sum_{i=1}^{2}\varepsilon_i\, v^i) & \text{if } f_1 \le f < f_2 \\ w_r\, \mathscr{L}(f, f_2, \sigma) & \text{if } f_2 \le f < f_3, \end{cases}$$

$$\Psi(f) \;\equiv\; 2\pi f t_0 + \varphi_0 + \frac{3}{128\eta v^5}\Big(1 + \sum_{k=2}^{7} v^k\, \psi_k\Big). \qquad (1)$$

In the above expressions, $f' \equiv f/f_1$, $v \equiv (\pi M f)^{1/3}$, $\varepsilon_1 = 1.4547\,\chi - 1.8897$, $\varepsilon_2 = -1.8153\,\chi + 1.6557$, C is a numerical constant whose value depends on the sky-location, orientation and the masses, $\alpha_2 = -323/224 + 451\,\eta/168$ and $\alpha_3 = (27/8 - 11\,\eta/6)\chi$ are the PN corrections to the Fourier domain amplitude of the ($\ell = 2, m = \pm 2$ mode) PN inspiral waveform [19], t_0 is the time of arrival of the signal at the detector and φ_0 the corresponding phase, $\mathscr{L}(f, f_2, \sigma)$ a Lorentzian function with width σ centered around the frequency f_2, w_m and w_r are normalization constants chosen so as to make $A(f)$ continuous across the "transition" frequencies f_2 and f_1, and f_3 is a convenient cutoff frequency such that the power of the signal above this frequency is negligible. The phenomenological parameters ψ_k and $\mu_k \equiv \{f_1 - f_{\rm LSO}^0, f_2 - f_{\rm QNM}^0, \sigma - f_{\rm QNM}^0/Q^0, f_3\}$ are written in terms of the physical parameters of the binary as:

$$\psi_k = \sum_{i=1}^{3}\sum_{j=0}^{N} x_k^{(ij)}\,\eta^i \chi^j\,, \quad \mu_k = \sum_{i=1}^{3}\sum_{j=0}^{N} \frac{y_k^{(ij)}\,\eta^i \chi^j}{\pi M}\,, \qquad (2)$$

where $N \equiv \min(3-i, 2)$ while $x_k^{(ij)}$ and $y_k^{(ij)}$ are tabulated in Table I. Figure 1 plots the values of ψ_k and μ_k estimated from the hybrid waveforms, as well as the fits given by Eq. (2).

We match these waveforms to 2PN accurate adiabatic inspiral waveforms in the test-mass limit. In the $\eta \to 0$ limit, the phenomenological parameters reduce to the following:

$$f_1 \to f_{\rm LSO}^0,\;\; f_2 \to f_{\rm QNM}^0,\;\; \sigma \to f_{\rm QNM}^0/Q^0,\;\; \psi_k \to \psi_k^0, \qquad (3)$$

where $f_{\rm LSO}^0$ and $f_{\rm QNM}^0$ are the frequencies of the last stable orbit [35] and the dominant quasi-normal mode, and Q^0 is the ringdown quality factor [36] of a Kerr BH with mass M and spin χ, while ψ_k^0 are the (2PN) Fourier domain phasing coefficients of a test-particle inspiralling into the Kerr BH, computed using the stationary-phase approximation [19].

The test-particle-limit waveforms suffer from two limitations: 1) we assume that the evolution of the GW phase at the merger and ringdown stages is a continuation of the adiabatic inspiral phase, and 2) in the absence of a reliable model for plunge, we approximate the amplitude of the plunge with $f'^{-2/3}\,(1+\sum_{i=1}^{2}\varepsilon_i\, v^i)$. Nevertheless, in the test-mass limit, it is expected that the signal will be dominated by the long inspiral stage (followed by a quick plunge and ringdown), and the inspiral is guaranteed to be well-modelled by our waveform family. More importantly, the imposition of the appropriate test-mass limit in our fitting procedure

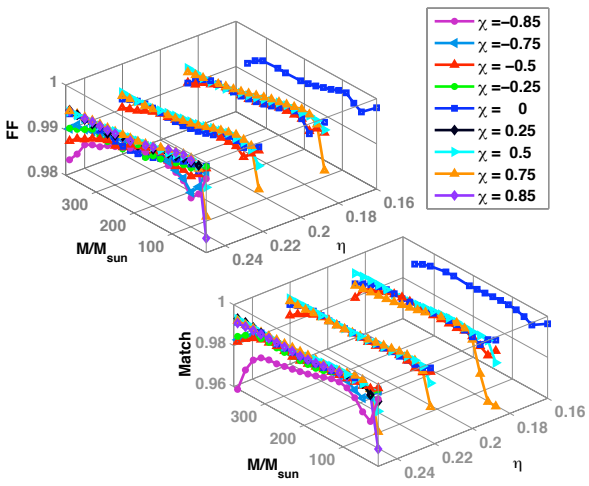

FIG. 2: Match and FF of the analytical waveforms with *equal-spin* hybrid waveforms constructed from simulation sets (1)–(3). M is the total mass, η is the symmetric mass ratio and χ the spin parameter.

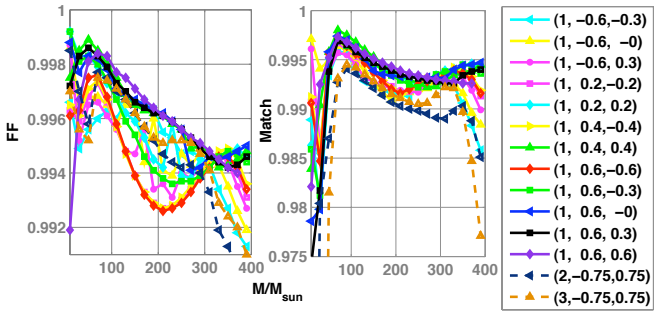

FIG. 3: Match and FF of the analytical waveforms with *unequal-spin* hybrid waveforms constructed from simulation sets (4) and (5). Parameters (q, χ_1, χ_2) of the hybrid waveforms are shown in legends.

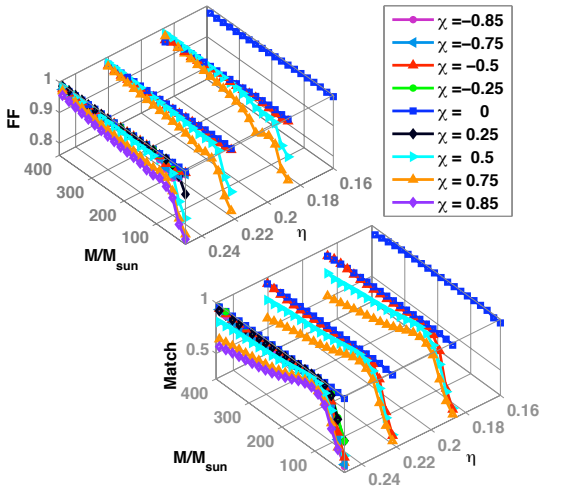

FIG. 4: Match and FF of *non-spinning* IMR templates proposed in [2, 7] with the equal-spin hybrid waveforms. A comparison with Fig. 3 demonstrates the effect of neglecting spins.

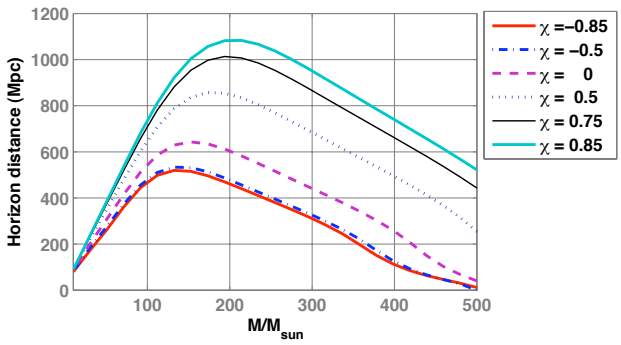

FIG. 5: Distance to optimally-located and oriented- equal-mass binaries with (equal) spin χ producing optimal SNR 8 in Initial LIGO.

ensures that the waveforms are well behaved even outside the parameter range where current NR data are available. Because of this, and the inclusion of the PN amplitude corrections, these waveforms are expected to be closer to the actual signals than the templates proposed in [2, 7] in the non-spinning limit (thus explaining the difference between the two waveform families).

We have examined the "faithfulness" of the new templates in reproducing the hybrid waveforms by computing the *match* (noise-weighted inner product) with the hybrids. Loss of the SNR due to the "mismatch" between the template and the true signal is determined by the match maximized over the whole template bank – called *fitting factor* (FF). The standard criteria for templates used in searches is that FF > 0.97, which corresponds to a loss of no more than 10% of signals.

Match and FF of the analytical waveforms with the equal- (unequal-) spin hybrid waveforms are plotted in Fig. 2 (Fig. 3), using Initial LIGO design noise spectrum [37]. Note that the analytical waveform family is constructed employing *only* the equal-spin hybrid waveforms. The PN–NR matching region used to construct the unequal-spin hybrids are also different from that used for equal-spin hybrids. These figures demonstrate the efficacy of the analytical templates in reproducing the target waveforms – templates are "faithful" (match > 0.97) *either* when the masses *or* the spins are equal, while they are *always* "effectual" in detection (FF > 0.97). These figures may be contrasted with Fig. 4, which details the effect of neglecting spin in the construction of the templates. This figure plots the matches of the non-spinning IMR template family proposed in [2, 7] with the equal-spin hybrid waveforms. FFs as low as 0.8 suggest that up to 50% binaries may go undetected if nonspinning IMR templates are employed to search for binaries with high spins (in the "hang-up" configuration), while matches as low as 0.3 suggest that the estimated parameters will be significantly biased.

Distance to optimally oriented BBHs (modeled by the new templates) producing optimal SNR of 8 at Initial LIGO noise spectrum is shown in Fig. 5, which demonstrates the dramatic effect of spin for detection of high-mass binaries; if most BBHs are highly spinning, then LIGO will be able to detect BH coalescences up to 1Gpc, thus increasing the event rates as much as five times compared to predictions based on models of nonspinning binaries. For Advanced LIGO, the distance reach is as high as 20 Gpc.

Conclusions.— We find that as many as 50% of signals may be missed when non-spinning IMR templates are used to search

	Test-mass limit (ψ_k^0)	$x^{(10)}$	$x^{(11)}$	$x^{(12)}$	$x^{(20)}$	$x^{(21)}$	$x^{(30)}$
ψ_2	$3715/756$	-920.9	492.1	135	6742	-1053	-1.34×10^4
ψ_3	$-16\pi+113\chi/3$	1.702×10^4	-9566	-2182	-1.214×10^5	2.075×10^4	2.386×10^5
ψ_4	$15293365/508032-405\chi^2/8$	-1.254×10^5	7.507×10^4	1.338×10^4	8.735×10^5	-1.657×10^5	-1.694×10^6
ψ_6	0	-8.898×10^5	6.31×10^5	5.068×10^4	5.981×10^6	-1.415×10^6	-1.128×10^7
ψ_7	0	8.696×10^5	-6.71×10^5	-3.008×10^4	-5.838×10^6	1.514×10^6	1.089×10^7
	Test-mass limit (μ_k^0)	$y^{(10)}$	$y^{(11)}$	$y^{(12)}$	$y^{(20)}$	$y^{(21)}$	$y^{(30)}$
f_1	$1-4.455(1-\chi)^{0.217}+3.521(1-\chi)^{0.26}$	0.6437	0.827	-0.2706	-0.05822	-3.935	-7.092
f_2	$[1-0.63(1-\chi)^{0.3}]/2$	0.1469	-0.1228	-0.02609	-0.0249	0.1701	2.325
σ	$[1-0.63(1-\chi)^{0.3}](1-\chi)^{0.45}/4$	-0.4098	-0.03523	0.1008	1.829	-0.02017	-2.87
f_3	$0.3236+0.04894\chi+0.01346\chi^2$	-0.1331	-0.08172	0.1451	-0.2714	0.1279	4.922

TABLE I: Phenomenological parameters describing the analytical waveforms (see Eq. (2)). In test-mass limit, they reduce to the appropriate quantities given by perturbative calculations [19, 35, 36]. The test-mass limit of f_1 is a fit to the frequency at the last stable orbit given in [35].

for binaries with non-precessing spins. To address the need for spinning IMR templates, we combine state-of-the-art results from analytical and numerical relativity to construct for the first time a family of analytical IMR waveforms for BBHs with non-precessing spins from "first principles". These templates do not contain unphysical parameters, and we show that for the purposes of GW detection it is sufficient to represent the spins by a single parameter. This will considerably simplify the use of our waveforms in GW searches in the near future, and will significantly accelerate the incorporation of NR results into the current effort for the first detection of GWs. There are many other immediate applications of our waveforms: injections into detector data will help to put more realistic upper limits on the rate of BBH coalescences [8, 9], and to compare the different algorithms employed in the search for BBHs [38], while employing these in population-synthesis studies will provide more accurate coalescence rates observable by the current and future detectors. Comparisons with precessing waveforms will help us to understand the implications of spin precession. Our method can readily be generalized to incorporate non-quadrupole spherical-harmonic modes, larger portions of the BBH parameter space and further information from analytical approximation methods or numerical simulations.

SH was supported in part as a VESF fellow of EGO, by DAAD grant D/07/13385 and grant FPA-2007-60220 from the Spanish Ministerio de Educación y Ciencia. MH was supported by SFI grant 07/RFP/PHYF148 and an FWF Lise Meitner fellowship (M1178-N16). PA and YC were supported in part by NSF grants PHY-0653653 and PHY-0601459, and the David and Barbara Groce Fund at Caltech. BB is supported in part by DFG grant SFB/Transregio 7 "Gravitational Wave Astronomy", BB and DM by the DLR, and LS by DAAD grant A/06/12630. We thank the Albert Einstein Institute, University of Jena, LRZ, ICHEC and CESGA for providing computational resources, and K. G. Arun, B. Sathyaprakash, G. Faye and R. O'Shaughnessy for useful discussions / comments.

[1] B. Sathyaprakash and B. Schutz, Liv. Rev. Relativity **12** (2009).
[2] P. Ajith et al., Phys. Rev. D **77**, 104017 (2008).
[3] P. Ajith and S. Bose, Phys. Rev. D **79**, 084032 (2009).
[4] A. Buonanno et al., Phys. Rev. D **76**, 104049 (2007).
[5] T. Damour and A. Nagar (2009), arXiv:0902.0136.
[6] P. Ajith et al., Class. Quant. Grav. **24**, S689 (2007).
[7] P. Ajith, Class. Quant. Grav. **25**, 114033 (2008).
[8] C. Robinson (2009), talk given at Amaldi Meeting, New York.
[9] C. Pankow et al. (2009), arXiv:0905.3120.
[10] A. Sesana et al., Astrophys. J. **698**, L129 (2009).
[11] M. Volonteri et al., Astrophys. J. **620**, 69 (2005).
[12] C. F. Gammie et al., Astrophys. J. **602**, 312 (2004).
[13] S. L. Shapiro, Astrophys. J. **620**, 59 (2005).
[14] C. Van Den Broeck et al. (2009), arXiv:0904.1715.
[15] P. Grandclement et al., Phys. Rev. D **69**, 102002 (2004).
[16] V. Kalogera, Pramana **63**, 673 (2004).
[17] T. Bogdanović et al., Astrophys. J. **661**, L147 (2007).
[18] C. Reisswig et al. (2009), arXiv:0907.0462.
[19] K. G. Arun et al., Phys. Rev. D **79**, 104023 (2009).
[20] M. Campanelli et al., Phys. Rev. Lett. **96**, 111101 (2006).
[21] J. G. Baker et al., Phys. Rev. Lett. **96**, 111102 (2006).
[22] B. Brügmann et al., Phys. Rev. D **77**, 024027 (2008).
[23] S. Husa et al., Class. Quant. Grav. **25**, 105006 (2008).
[24] D. Pollney et al., Phys. Rev. D **76**, 124002 (2007).
[25] S. Brandt and B. Brügmann, Phys. Rev. Lett. **78**, 3606 (1997).
[26] M. Hannam et al., Phys. Rev. Lett. **99**, 241102 (2007).
[27] S. Husa et al., Phys. Rev. D **77**, 044037 (2008).
[28] B. Brügmann et al., Phys. Rev. D **77**, 124047 (2008).
[29] M. Hannam et al., Phys. Rev. **D79**, 084025 (2009).
[30] M. Hannam et al., Phys. Rev. D **78**, 104007 (2008).
[31] M. Hannam et al. (2009), in preparation.
[32] T. Damour et al., Phys. Rev. D **63**, 044023 (2001).
[33] L. Blanchet et al., Phys. Rev. Lett. **93**, 091101 (2004).
[34] L. Blanchet et al., Class. Quant. Grav. **25**, 165003 (2008).
[35] J. M. Bardeen et al., Astrophys. J. **178**, 347 (1972).
[36] F. Echeverria, Phys. Rev. D **40**, 3194 (1989).
[37] http://www.ligo.caltech.edu/∼jzweizig/distribution/LSC_Data.
[38] B. Aylott et al., Class. Quantum Grav. **26**, 165008 (2009).